

## **SUPPLEMENTAL MATERIAL**

### **Imaging high-risk atherothrombosis using a novel fibrin-binding PET probe**

David Izquierdo-Garcia, PhD<sup>1,2</sup>, Himashinie Diyabalanage, PhD<sup>3</sup>, Ian A. Ramsay, BS<sup>1,3,4</sup>,  
Nicholas J. Rotile, BA<sup>1,4</sup>, Adam Mauskapf, BS<sup>5</sup>, Ji-Kyung Choi, PhD<sup>1</sup>, Thomas Witzel, PhD<sup>1</sup>,  
Valerie Humblet, PhD<sup>3</sup>, Farouc A. Jaffer, MD PhD<sup>5</sup>, Anna-Liisa Brownell, PhD<sup>6</sup>, Ahmed Tawakol,  
MD<sup>7</sup>, Ciprian Catana, MD PhD<sup>1,4</sup>, Mark F. Conrad, MD<sup>8</sup>, Peter Caravan, PhD<sup>1,4\*</sup>, Ilknur Ay, MD  
PhD<sup>1\*</sup>

<sup>1</sup>Athinoula A. Martinos Center for Biomedical Imaging, Department of Radiology, Massachusetts  
General Hospital and Harvard Medical School, Charlestown, MA

<sup>2</sup>Harvard-MIT Department of Health Sciences and Technology, Massachusetts Institute of  
Technology, Cambridge, MA

<sup>3</sup>Collagen Medical, LLC, Belmont, MA

<sup>4</sup>The Institute for Innovation in Imaging, Department of Radiology, Massachusetts General  
Hospital, Charlestown, MA

<sup>5</sup>Cardiovascular Research Center, Division of Cardiology, Department of Medicine  
Massachusetts General Hospital and Harvard Medical School, Boston, MA

<sup>6</sup>Gordon Center for Medical Imaging, Department of Radiology, Massachusetts General  
Hospital and Harvard Medical School, Charlestown, MA

<sup>7</sup>Nuclear Cardiology, Division of Cardiology, Department of Medicine, Massachusetts General  
Hospital and Harvard Medical School, Boston, MA

<sup>8</sup>Division of Vascular and Endovascular Surgery, Massachusetts General Hospital and Harvard  
Medical School, Boston, MA

## SUPPLEMENTAL METHODS

### ***Synthesis of fibrin specific probe $^{68}\text{Ga}$ -CM246 and nonbinding isomer $^{68}\text{Ga}$ -CM249***

Reagents: All chemicals were purchased commercially (Sigma-Aldrich, Fisher Scientific, EMD, BDH, Biotage) and used without further purification.

Probe synthesis:  $^{68}\text{Ga}$ -CM246 comprises a short, cyclic fibrin-specific peptide conjugated to a Ga-68 chelate. The probe was designed based on a known fibrin binding peptide previously employed in the MR probe EP-2104R, which was shown to specifically detect fibrin/thrombus in humans and animal models<sup>41,43,46</sup>. A D-cysteine non-binding control probe,  $^{68}\text{Ga}$ -CM249, was prepared by changing the chirality of a key amino acid to eliminate fibrin binding. In detail,  $^{68}\text{Ga}$ -CM246 (or  $^{68}\text{Ga}$ -CM249) was synthesized by first conjugating the NHS-activated ester of tert-butyl protected NODAGA to a cyclic, disulfide bridged 11-amino acid fibrin-binding peptide. The tert-butyl groups were removed by treatment with a solution of trifluoroacetic acid (TFA), methanesulfonic acid, 1-dodecanethiol, and H<sub>2</sub>O (92:3:3:2) while monitoring the reaction by LC-MS, followed by the addition of cold diethyl ether to precipitate the product. For radiochemical synthesis of  $^{68}\text{Ga}$ -CM246 and  $^{68}\text{Ga}$ -CM249,  $^{68}\text{GaCl}_3$  (1 mCi, in 0.5 mL HCl (0.6 M)) was diluted with pH 5, 3M sodium acetate (200  $\mu\text{L}$ ) to reach pH 4.1.  $^{68}\text{GaCl}_3$  solution (200  $\mu\text{L}$ ) was combined with each NODAGA-Peptide (0.1 mM 10  $\mu\text{L}$ ) solution in sodium acetate (10 mM, pH 4.1), and the reaction mixture was heated at 60 °C for 10 min and purified by Sep-Pak light C18 cartridge (Waters) to remove any radiometal impurities (germanium-68 breakthrough). The radiochemical purity of the final solutions of the  $^{68}\text{Ga}$ -CM246 and  $^{68}\text{Ga}$ -CM249 were  $\geq 95\%$ , as determined by radio-HPLC analyses.

### ***Pharmacokinetics of $^{68}\text{Ga}$ -CM246 in healthy rabbits***

Four healthy New Zealand white rabbits were anesthetized with ketamine/xylazine (35 mg/kg/3.5 mg/kg, IM) for induction and isoflurane (1-2% in medical air) for maintenance. The

right marginal ear vein was cannulated for injection of the  $^{68}\text{Ga}$ -CM246. The right femoral artery was cannulated for blood collection at 0, 2, 5, 10, 15, 30, 60, 90, and 120 minutes post-injection (p.i.) using EDTA tubes. Blood clearance was determined by weighing each arterial blood sample and counting using a gamma counter (Wizard2, Perkin Elmer) along with an aliquot of the injected dose. The activity was expressed as percent injected dose (%ID) per gram of blood. Also, the 0-, 10-, 60-minute blood samples were used for the functional probe assay, and the 0-, 15-, 90-minute samples were utilized for radio-HPLC analysis for metabolites. Rabbits were euthanized at the end of the 2 hours, and the organs were removed, weighed, and counted using a gamma counter to determine biodistribution. The activity in the organs was expressed as %ID per gram of tissue.

*Functional probe assay:* Fibrin plates were prepared as follows: Human fibrinogen (1 g) was dissolved in 30 mL of TBS buffer (50 mM Tris, 150 mM NaCl, 5 mM sodium citrate, pH 7.4) and dialyzed in a Slide-a-Lyzer (20 000 MWCO, Cassette G2) at room temperature. After two changes of the buffer, the fibrinogen was centrifuged (10 min,  $2000 \times g$ ) to remove undissolved material. Fibrinogen concentration was determined by measuring the absorbance at 280 nm: a 1 mg/mL solution has an absorbance of 1.512 OD units. Stock fibrinogen solution concentration was 32.1 mg/mL. Fibrin plates with alternating rows of clotted fibrin and empty wells were prepared by polymerizing fibrinogen (100  $\mu\text{L}$ ; 2.5 mg/mL) with thrombin (1 U/mL) in TBS•citrate supplemented with 7 mM  $\text{CaCl}_2$  in the wells of a 96 well polystyrene microtiter plate (Immulon-II®). The plates (un-covered) were dried overnight at 37 °C to a thin film, which adsorbs to the plate and then sealed with tape and stored at  $-20$  °C until use. Clottable protein in individual fibrinogen batches was determined by measuring 280 nm absorbance of the soluble fraction of the solution before and after thrombin treatment and was generally  $\geq 96\%$  (Fibrin concentration, 7.56  $\mu\text{M}$ ).

Blood samples were centrifuged for 10 min at 4950 rpm (2000 g) to separate plasma. Plasma (150  $\mu$ L) was pipetted into an Eppendorf tube (500  $\mu$ L), and TBS buffer (150  $\mu$ L) was added. A control sample was prepared by adding the probe (5  $\mu$ L) into the plasma taken at  $T=0$ . Each sample (100  $\mu$ L) was added to two wells, one containing immobilized fibrin and an empty well. The sample plates were covered, placed on a shaker, and incubated at room temperature for 45 min. After incubation, an aliquot (90  $\mu$ L) was carefully pipetted out into a pre-weighed test tube from the supernatant of each well. The activity of each was measured using a gamma counter. By measuring the activity in a well plate containing fibrin and comparing it to the activity in a well plate without fibrin, the percentage of activity bound to fibrin was estimated. This %bound is compared to the %bound measured when a pure probe is spiked into fresh plasma. The ratio of %bound measured at time  $t$  to %bound at  $t = 0$  provides a measure of the percentage of activity present as a fibrin binding probe.

*Radio-HPLC analysis of blood for metabolites:* Plasma (100  $\mu$ L) was added to cold acetonitrile (100  $\mu$ L) and placed in an ice bath for 10 min. The samples were centrifuged (for 10 min at 4950 rpm), the supernatant was separated and passed through a 0.22- $\mu$ m Millipore filter. Aliquots (50  $\mu$ L) of samples were injected onto an analytical HPLC column (method A595HD.M), and the eluent was collected every 0.5 min. All fractions were counted by a gamma counter, and data were plotted to reconstruct the HPLC chromatograms. The obtained data were compared to that of the pure probe injected onto the same column to identify the number of metabolites and the fraction of the intact probe circulating at each time point.

### ***Rabbit model of atherosclerosis and plaque rupture***

Adult male and female New Zealand white rabbits (N=13; 2.8-4.0 kg; Charles River Laboratories) were fed with 1% cholesterol and 4.7% coconut oil high cholesterol diet (HCD; Research Diets, Inc., New Brunswick, NJ) for eight weeks followed by four weeks of a regular diet. Two weeks after the initiation of HCD, rabbits were anesthetized (ketamine/xylazine

followed by isoflurane). A 3F Fogarty balloon catheter was inserted into the caudal 6 cm of the abdominal aorta under fluoroscopic guidance to induce endothelial denudation and atherosclerotic plaque formation. At the end of the 12 week diet period, rabbits were re-anesthetized, animals allocated to the plaque rupture group (n=9) were injected with Russell's viper venom (0.15 mg/kg, IP) and histamine (0.02 mg/kg; IV), whereas control rabbits (n=4) received no injection. After cannulation of the right marginal ear vein, rabbits were placed in the PET/MR scanner.

*Fibrin-binding probe injection and PET/MR image acquisition:* Immediately after the surgical procedures, animals were placed in a combined brain PET-3T MR system (Siemens Medical Solutions) and were injected with  $^{68}\text{Ga}$ -CM246 (2.4 – 5.6 MBq/kg; IV). The total activity injected was calculated by subtracting the activity in the syringe before injection from the activity remaining in the syringe after injection as measured by a dose calibrator (Capintec CRC-25PET). All doses were decay corrected to the time of injection. For the first three animals, PET images were acquired dynamically from time of injection out to 150 min. After establishing an optimal imaging time, subsequent PET images were acquired for 90 min in listmode, from 50 to 135 min post-injection (p.i.).

For MR imaging, an in-house built surface coil in conjunction with a birdcage 8-channel head coil (Siemens Healthineers, Erlangen) was used. Three MR images were acquired simultaneously during the PET acquisition: (1) a magnetization prepared rapid-gradient echo (MPRAGE) used for global anatomical localization and attenuation correction purposes, (2) a dark-blood T2 sequence used to provide high-resolution images of the atherosclerotic plaques, and (3) a time-of-flight (ToF) sequence used to provide good localization of the whole abdominal aorta from the renal to the iliac bifurcations.

*PET image reconstruction:* In vivo PET images were reconstructed in 15-minute frames using a 3D OP-OSEM algorithm with 6-iterations and 16 subsets and applying corrections for

attenuation, scatter, random prompts, normalization, dead-time, decay, and background. PET images were reconstructed into a 344×344×152 matrix with 1.25 mm<sup>3</sup> isotropic voxel size. Attenuation correction was performed using the MPRAGE image to segment the whole-body contour and assigning a linear attenuation coefficient (LAC) of 0.096 cm<sup>-1</sup>, similar to what is currently done in Whole-Body PET/MR scanners. We had previously shown that for tracers with comparable uptake in the aorta as FDG, the bias introduced by the attenuation is less than 5% .

*Ex vivo PET imaging and autoradiography:* Immediately after in vivo imaging, animals were euthanized under deep anesthesia using potassium chloride solution (2 mEq/kg; IV). The abdominal aorta (from the renal to the iliac bifurcation), the inferior vena cava, and the right common carotid artery were harvested for ex vivo PET imaging, autoradiography, gross pathology, and histology using Carstairs' staining. Ex vivo PET imaging was started 200 ± 25-min p.i., and autoradiography started 260 ± 35-min p.i. PET images were reconstructed into a single 20-minute frame using a similar algorithm and correction methods as for the in vivo case. Autoradiography was done using a multipurpose film and a Perkin-Elmer Cyclone Plus Storage Phosphor Imager. The exposure time was 30 minutes.

*Gross pathology and histology:* Immediately after autoradiography, the abdominal aorta was cut into four equal length segments and fixed using 4% paraformaldehyde containing 30% sucrose. Each segment's rostral part was embedded in an optimal cutting temperature compound for cryosectioning for histology (Carstairs' staining). The remaining aortic segments were cut open for gross pathology to detect thrombus formation in the aortic lumen. Carstairs' staining of the rabbit abdominal aorta sections (10 μ m-thick) was used to differentiate fibrin (bright red), collagen (bright blue), erythrocytes (yellow to orange), platelets (gray-blue to navy), and muscle (red)<sup>55</sup>. Sections were inspected using a microscope (Nikon Eclipse 50i, Kodak Scientific Imaging System), and digital images were acquired using a camera (SPOT 7.4 Slider RTKE,

Diagnostic Instruments) connected to a computer. Whole slides were scanned using a NanoZoomer-SQ Digital slide scanner (Hamamatsu Photonics K.K., Japan).

### ***Ex vivo studies of human carotid endarterectomy specimens***

Freshly discarded surgical specimens were embedded in optimal cutting temperature compound, snap-frozen, and stored at -80 °C before further analysis. Alternating consecutive cryosections were processed for histology and autoradiography; triplicate tissue samples with a 50 µm gap in between were used for these experiments. The remaining tissue samples were processed for functional probe assay. For histology, Carstairs' staining was used as described in the rabbit experiments section. For autoradiography, three 30 µm-thick sections were incubated with <sup>68</sup>Ga-CM246 or D-cysteine non-binding control probe <sup>68</sup>Ga-CM249 for 45 minutes on a lab shaker at room temperature. Autoradiography was performed after three washes of PBS. The exposure time was 2 minutes.

For the probe binding assay, samples were thawed at room temperature, weighed (8-15 mg per sample), cut into duplicates, and placed into tubes containing 110-150 kBq (3-4 µCi) <sup>68</sup>Ga-CM246 or control probe <sup>68</sup>Ga-CM249 in 1 mL PBS. The mixture was shaken for 45 minutes at room temperature. After centrifugation, supernatant (sup-1) was removed, kept for further analysis, and tissue samples were washed with PBS (1 mL); this procedure was repeated twice for each sample. Wash solutions (wash-1 and wash-2) were kept for further analysis. Activities in tissue samples and solutions sol-1, wash-1, and wash-2 were measured on a gamma counter. Percent uptake was calculated as follows:

$$\% \text{ uptake} = [(\text{activity in tissue}) / \text{total activity (tissue + sup-1 + wash-1 + wash-2)}] \times 100$$

### ***Data analysis***

Rabbits allocated into the plaque rupture group but had no thrombus at all in gross pathology were pooled with control group rabbits for data analysis.

Analysis of the abdominal aorta, from the renal to the iliac bifurcation, was divided into four equal length segments (~2 cm). Regions of interest (ROIs) were semi-automatically obtained from the axial views of the ToF MR images (for in vivo results) or directly from the ex vivo PET images (for ex vivo results), with manual adjustments if required. Background ROIs were drawn on the back muscles (the longissimus and the iliocostalis), using circular ROIs of 40 voxel diameter, on at least 10-consecutive axial slices. PET images were then resliced into the MR space, and ROIs were applied into the resliced PET images. Results are reported in two different manners: *per-segment*, averaging the ROIs' results on each quarter; and *per-animal*, averaging all ROI values across all four segments of the abdominal aorta. For both in vivo and ex vivo images, PET values were obtained as mean and maximum standardized uptake values (SUV and SUV<sub>max</sub>, respectively)<sup>18</sup>. Additionally, for in vivo images, tissue to background ratios (TBR) and maximum TBR (TBR<sub>max</sub>) were calculated using the background ROI to normalize radiotracer clearance across animals.

During ex vivo PET image analysis, to minimize the impact of partial volume effect (PVE) errors, the ROIs were drawn slightly larger than the actual diameter of the aorta, and accumulated SUV values were then calculated per ROI.

Autoradiography data from rabbits were quantified using PerkinElmer OptiQuant 5.0 software. Four ROIs were drawn around each quarter of the aorta for the per-segment analysis, and a single ROI covering the whole aorta was used for the per rabbit analysis. ROIs for the inferior vena cava and the carotid artery were drawn around the entire tissue. Results were measured as digitalized light units per mm<sup>2</sup> (DLU/mm<sup>2</sup>). Autoradiography from human specimens was quantified using Image J (NIH) to calculate the mean intensity (integrated density divided by the area) for each section; measurements from triplicate sections were averaged to calculate the mean value for each patient.



The gross pathology of each segment was scored as thrombus-negative or thrombus-positive. Rabbits with at least one thrombus-positive aortic plaque segment in gross pathology were assigned to the thrombosis group. In contrast, animals that had no thrombus were assigned to the non-thrombosis group. Overall, gross pathology defined the gold standard of plaque thrombosis for comparison of results.

Per-segment and per-animal results were obtained for the in vivo PET, ex vivo PET, and autoradiography data as defined above. ROC curves were used to identify the best thresholds to define plaque rupture using in vivo PET results vs. the gold standard.

### ***Statistical analysis***

Differences between groups were compared using linear models, as follows: (1) all ruptured vs. non-ruptured comparisons for the per-animal analysis were performed using a linear regression model; (2) for the per-segment analysis, differences between groups were analyzed using a linear mixed-effects model with the dichotomous variable of histology defining rupture as the fixed effect and random effect for the intercept to account for the potential correlation across segments for the same animal and; (3) a linear regression model was used to compare the in vivo PET imaging values between the aorta and the muscle ROIs, controlling for the group (ruptured vs. non-ruptured).

### **SUPPLEMENTAL RESULTS**

To confirm that the inclusion of the two non-triggered rabbits does not change the statistical results of the in vivo group analysis, we have performed group comparison with and without the two non-triggered animals included as part of the control group. The results showed almost identical statistics, demonstrating no changes in the group results and analysis (Table I).

### Supplemental Table

**Table I:** Statistics for the group comparisons (p-values) with and without the two non-triggered animals as part of the Control group.

	SUV	SUVmax	TBR	TBRmax
Including Non-triggered	0.21	0.19	0.038*	0.036*
Excluding Non-triggered	0.2	0.17	0.034*	0.04*

## Supplemental Figures and Figure Legends

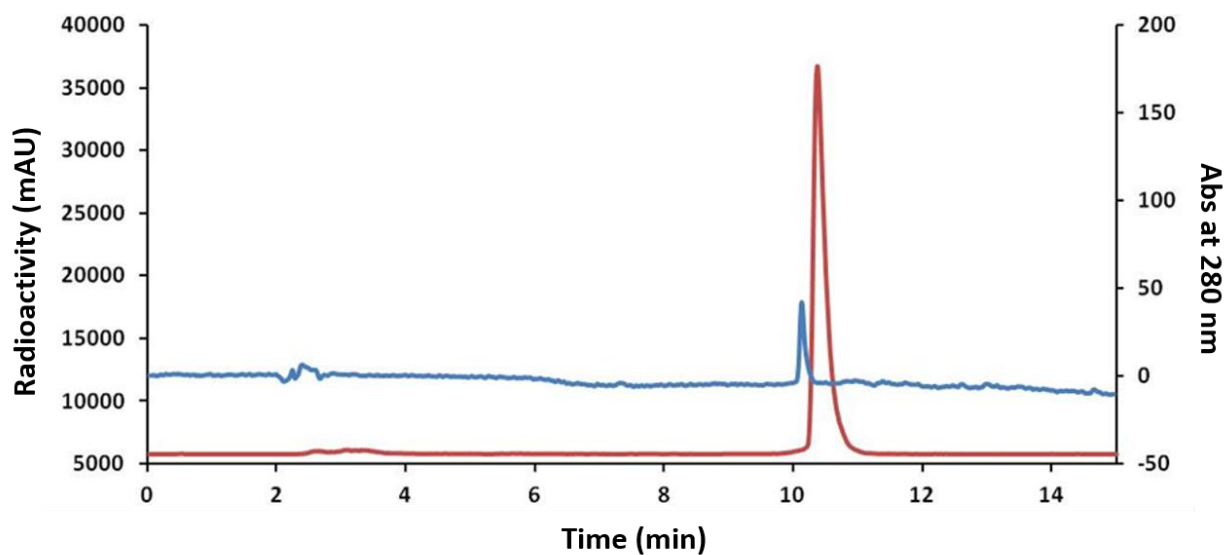


**Figure I.** HPLC traces for  $^{68}\text{Ga}$ -CM246. Radio-HPLC trace in red shows the radiochemical purity of  $^{68}\text{Ga}$ -CM246, and blue shows UV detection trace of non-radioactive pure compound. The radioactivity detector was positioned after the UV detector, resulting in an offset in retention times between the UV trace and the radioactivity trace.

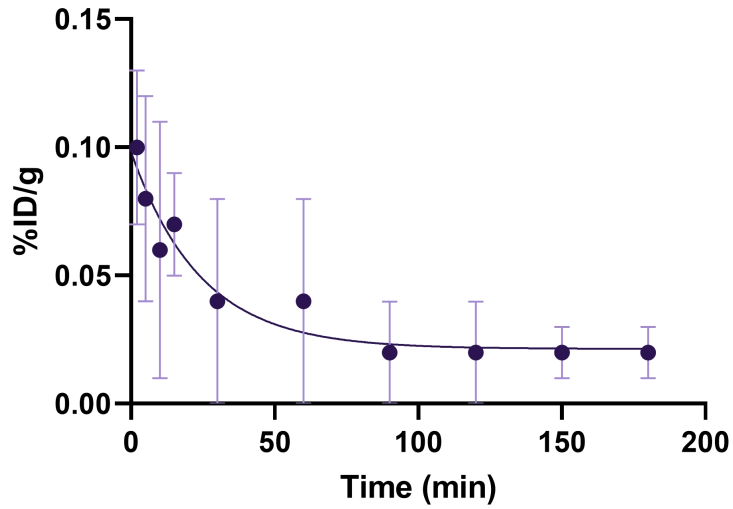


**Figure II.** Blood clearance of  $^{68}\text{Ga}$ -CM246 expressed as percent injected dose per gram of blood (%ID/g) in healthy control rabbits (n=3) showed a rapid clearance with a half-life of 23 minutes.

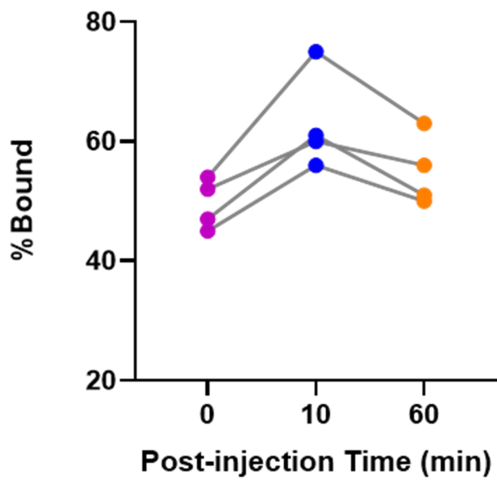


**Figure III.** Percentage of probe bound to fibrin before (T=0) or after injection into healthy rabbits at T = 10 and 60 min showed that the probe  $^{68}\text{Ga}$ -CM246 is intact and functional at both time points post-injection.

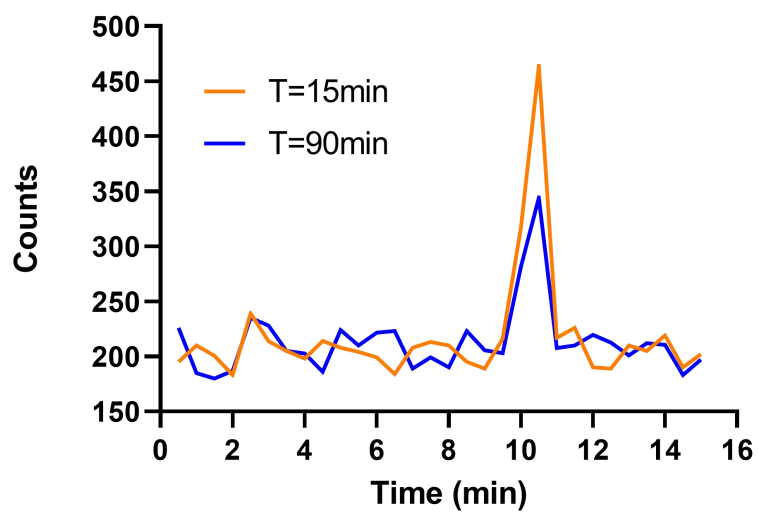


**Figure IV.** Representative examples of radio-HPLC traces obtained from a healthy rabbit showing remaining intact probe at T=15 min and T=90 min post-injection demonstrated the metabolic stability of the probe  $^{68}\text{Ga}$ -CM246.

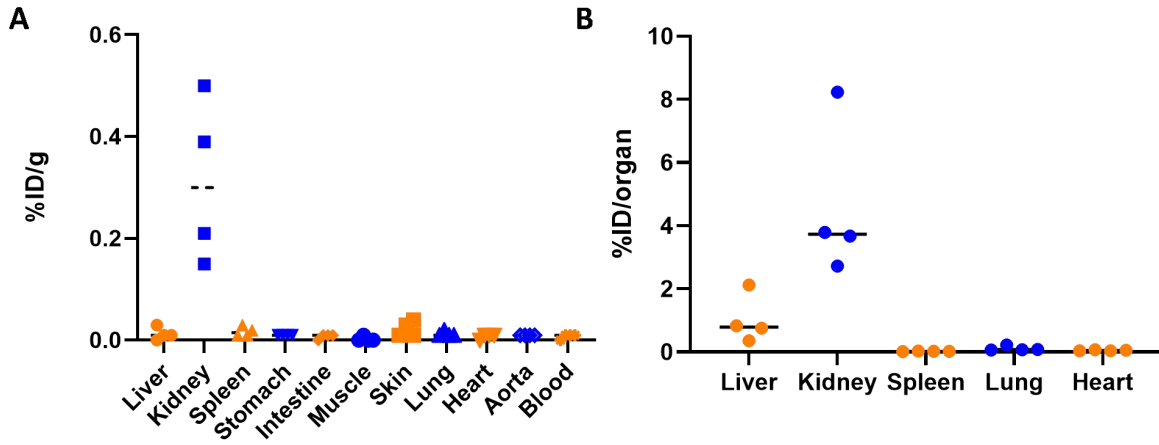


**Figure V.** Ex vivo activity in tissues as (A) percent injected dose per gram (%ID/g) and (B) percent injected dose per organ (%ID/organ) in healthy control rabbits (n=4) euthanized 120 min post-injection showed that most of the probe is eliminated from the animal.

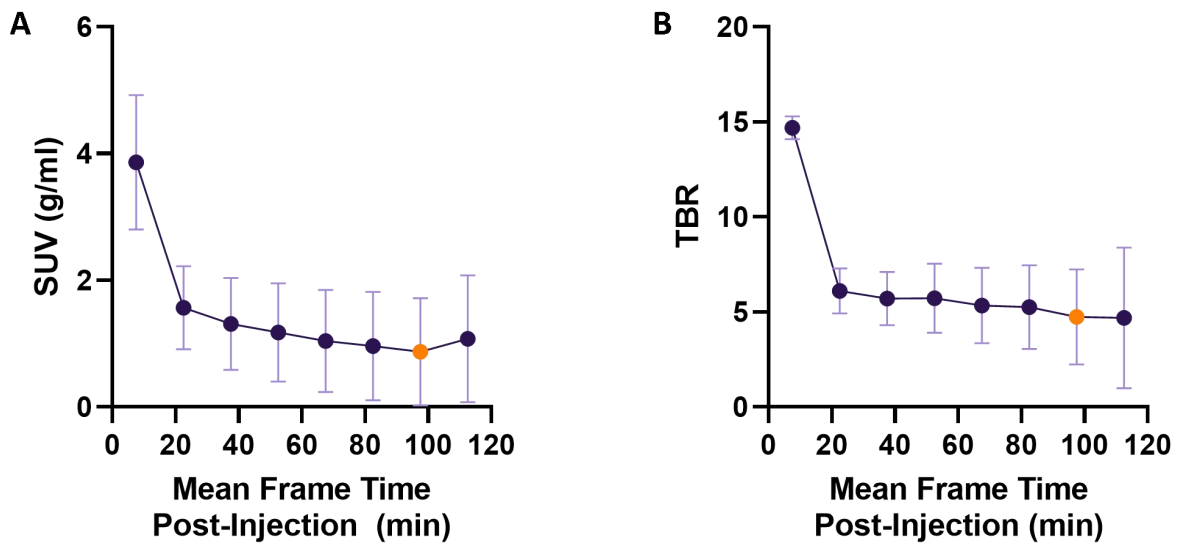


**Figure VI.** Time activity curves (TACs) of the first three rabbits that had imaging from the start of the  $^{68}\text{Ga}$ -CM246 PET radiotracer injection up to 120 min post-injection. (A) Aorta SUV, (B) Aorta-to-muscle ratio (TBR). The best imaging time point was chosen at 90-105 min post-injection (orange dots), where both curves flatten.



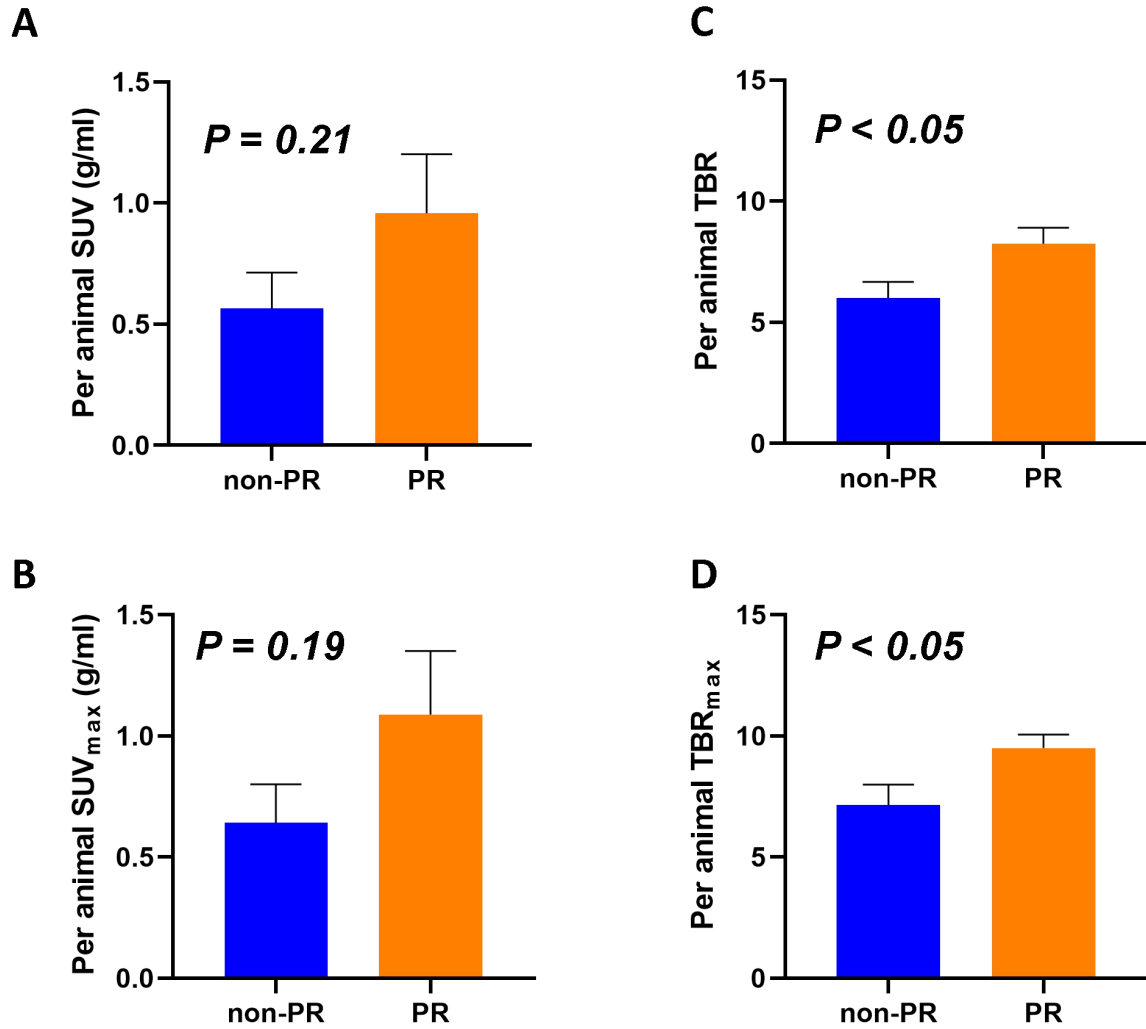
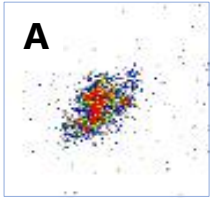
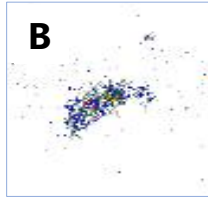


**Figure VII.** In vivo PET data calculated as per-animal comparing probe uptake in the abdominal aorta in the plaque rupture (PR) group vs. non-plaque rupture (non-PR) group. Data were expressed as SUV (A) and SUV<sub>max</sub> (B), the aorta to muscle ratio, TBR (C), and TBR<sub>max</sub> (D).

**[<sup>68</sup>Ga]CM-246**  
Fibrin-binding probe



**[<sup>68</sup>Ga]CM-249**  
Non-binding probe



Carstairs' staining

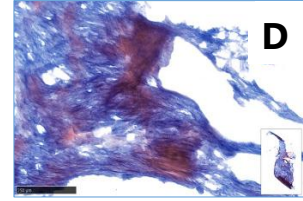
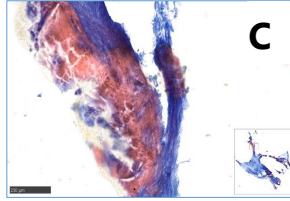


**Figure VIII.** Representative autoradiography (A-B) and light microscopy images of Carstairs' stained sections (C-D) from patient specimens with low <sup>68</sup>Ga-CM246 uptake.